Multistability resulting from random rearrangements in a ring resonator with a nonlinear element

V. V. Zverev and B. Y. Rubinshtein

Opt. Spectrosc. (USSR) **62**(4), April 1987

Abstract

Certain types of random rearrangements of attracting sets (attractors) arising in the phase space of a ring resonator containing a nonlinear medium are studied numerically. It is shown that for certain values of the parameters we can reduce the 2-D mapping describing the evolution of the field in the resonator to 1-D and give a qualitative explanation of the threshold phenomena observed. A method is considered for expansion in terms of a small parameter that allows us to calculate the fine structure of a random attractor analytically.

As it has been shown in [1] - [5], self-oscillations transformed into random motion (optical turbulence) can arise in a ring resonator with a nonlinear element (henceforth to be called the nonlinear ring resonator – NRR). This paper is devoted to the study of random rearrangements of attractors in the phase space of the NRR (including random-regular motion transitions), leading to behavior similar to hysteresis. Such behavior was observed in the numerical modeling of NRR dynamics in the adiabatic regime (the Ikeda mode [1]); it was assumed that nonlinear conversion of light takes place due to the ν-photon transitions in the two-level medium. It is important that at the time of rearrangements of an attractor, an exchange (jump) of the type of NRR dynamics takes place; such a transition can result both in the smooth variation of some parameter of the system and in impulse perturbation of the exciting field. This indicates, in principle, feasibility of the design of new types of multistable (having a series of stable states) optical devices based on NRR (we call multistable dynamic systems or states, to which correspond before and after the jump isolated attracting sets, but stationary points are optional).

We consider a theoretical NRR model. Let a two-level medium placed in the ring resonator be excited by an external light source (stationary and coherent) through a beam splitter; after passing through the active medium part of the light leaves the resonator through another beam splitter; the intensity reflectance of each of the mirrors is equal to κ.

In the case of ν-photon transitions, the slowly varying electric field amplitude $\mathcal{E}$ of the wave, the polarization P of the medium, and the density W of population inversion satisfy the equations

$$\mathcal{E}' + c^{-1}\dot{\mathcal{E}} = i\beta g P^* (\mathcal{E}^*)^{\nu-1}, \tag{1}$$

$$\dot{P} = -\frac{P}{T_2} + i(\omega_0 - \nu\omega)P + ig(\mathcal{E}^*)^\nu W, \tag{2}$$

$$\dot{W} = -\frac{1+W}{T_1} + i(g^*\mathcal{E}^\nu P - c.c.)/2, \tag{3}$$

where c is the speed of light; T_1 is the energy relaxation time; T_2 is the dephasing time; ω_0 is the resonant frequency of the medium; ω is the frequency of the exciting field; g and β are constants

characterizing the medium; derivatives with respect to z and time t are denoted by prime and dot, respectively. For $T_2 \ll T_r$, where T_r is resonator round trip time, the NRR dynamics (in the traveling-wave regime) can be described by a set of differential-difference equations

$$\dot{\Psi}(t) = -\frac{\Psi(t)+1}{T_1} + (2\beta l_0)^{-1} \mid \mathcal{E}(t-T_r) \mid^2 [1-\exp(2\chi_\nu(t))], \tag{4}$$

$$\mathcal{E}(t) = \sqrt{1-\kappa}\,\mathcal{E}_{ex} + \kappa \mathcal{E}(t-T_r)\exp[(1-i\delta)\chi_\nu(t) + i\theta], \tag{5}$$

where

$$\chi_1(t) = \beta l_0 \mid g \mid^2 \Psi(t) T_2/(1+\delta^2), \tag{6a}$$

$$\chi_\nu(t) = -\frac{1}{2(\nu-1)} \ln\left\{1 - \frac{2(\nu-1)\beta l_0 \mid g \mid^2 T_2}{1+\delta^2} |\mathcal{E}(t-T_r)|^{2\nu-2}\Psi(t)\right\}, \quad \nu > 1; \tag{6b}$$

$$\Psi(t) = \frac{1}{l_0}\int_0^{l_0} W(t-T_r+z/c, z)dz, \tag{7}$$

$T_r = l/c,\ \delta = (\omega_0 - \nu\omega)T_2,\ \theta = (\omega-\omega_c)T_r,\ l_0$ is length of the active region of the NRR, l is the total resonator length, ω_c is the frequency of the isolated mode of the field, $\mathcal{E}_{ex}$ and $\mathcal{E}(t)$ are complex amplitudes of the electric field of the exciting wave and wave at the entrance to the active medium, respectively. We omit a detailed description of the procedure for deriving Eqs.(4)-(6b), discussed in [3] for $\nu = 2$ and is easily generalized to the case of arbitrary ν. By assuming additionally that $\beta l_0 |g|^2 T_2/(1+\delta^2)|\mathcal{E}|^{2\nu-2}\Psi \ll 1,\ \delta \gg 1,\ T_1 \ll T_r$, we can describe the dynamics of the NRR by 2-D mapping

$$E_{N+1} = E_{ex} + \kappa E_N \exp\left[\frac{i\theta + iR|E_N|^{2\nu+2}}{1+|E_N|^{2\nu}}\right], \tag{8}$$

where $E_N = \sqrt{\alpha}\mathcal{E}(NT_r), E_{ex} = \sqrt{\alpha(1-\kappa)}\mathcal{E}_{ex}, R = \beta l_0 \delta\alpha/T_1, \alpha = (|g|^2 T_1 T_2/(1+\delta^2))^{1/\nu}$. We imply using Eq. (8) that the amplitude of the field at the entrance to the active medium changes abruptly at $t = NT_r$, where $N = 1, 2, 3, \ldots$, and remains constant during each time interval $NT_r < t < (N+1)T_r$; thus, the phase trajectory of the NRR (in discrete time scale) is obtained as a result of iteration of mapping (8). In this paper, we will consider only the dynamics of mapping.

We note that for $\nu = 1, |E_N| \ll 1$, a simpler mapping is derived from Eq. (8)

$$E_{N+1} = E_{ex} + \kappa E_N \exp\left(i(\theta - R) - iR|E_N|^2\right), \tag{9}$$

it was studied in [1, 2]. By representing the results of iteration of mapping (8) by points in the complex E plane, we can observe different types of NRR dynamics: convergence of the sequence of points to a limiting (stationary) point; convergence to each j-th group of points ($j = 1, 2, \ldots, H$), including points with numbers $N = j + HK, K = 0, 1, 2, \ldots$, to its limit (cycle of multiplicity H); random motion. In the last case the points form an image of random (strange) attractor (SA), normally having the form of a thick curve or a set of curves. By considering an enlarged fragment of such curve, we can discover that it consists of several close quasiparallel curves (first-order fine structure); each of these curves in turn possesses a similar second-order structure, and so on. Thus, the SA of mapping (8) is sturturally similar to the Henon attractor described in [7], and is the direct product of a 1-D manifold and the Cantor set (also see [1] and [3]). For certain combinations of the values of the NRR parameters, we can analyze the SA structure by reducing the 2-D mapping (8) to approximate 1-D mapping. The

method of reduction [8] is a modification of the method used earlier in [6] for SA of polynomial mappings. Introducing polar coordinates $E_N - E_{ex} = r_N \exp(i\Phi_N)$, we rewrite Eq. (8) in the form

$$\begin{aligned} r_{N+1} &= \kappa|E_{ex} + r_N \exp(i\Phi_N)|, \\ \Phi_{N+1} &= \Phi^I_{N+1} + \Phi^{II}_{N+1} + \theta, \end{aligned} \tag{10}$$

where

$$\begin{aligned} \Phi^I_{N+1} &= \arg(E_{ex} + r_N \exp(i\Phi_N)), \\ \Phi^{II}_{N+1} &= G(r_{N+1}/\kappa), \quad G(w) = \frac{Rw^{2\nu+2}}{1+w^{2\nu}}. \end{aligned} \tag{11}$$

We may assume E_{ex} is real. We note that it follows from Eq. (10) that $r_{N+1} \le \kappa(E_{ex}+r_N)$ (the triangular inequality) due to the fact that $r_N \le r_M = \kappa E_{ex}(1-\kappa)$, where r_M is a stationary point dominating the mapping $r_{N+1} = \kappa(E_{ex} + r_N)$; so that the sequence $\{r_N\}$ is finite. Using this, we can show that for $\kappa \ll 1$ the following estimates are valid

$$|\Phi^I_N| \le r_M/E_{ex} \sim \kappa, \quad |\Phi^{II}_N| \sim G(E_{ex}), \tag{12}$$

and, if furthermore, $E_{ex} \sim R \sim 1$, then $|\Phi^I_N| \ll |\Phi^{II}_N|$; this inequality can be satisfied also for other combinations of the parameter values. By taking Φ^I_N to be small, we introduce the formal expansion parameter $\Phi^I_N \to \epsilon\Phi^I_N$ and seek an equation of SA as the equation of a family of invariant curves of mapping (10), by representing the r.s.h. of this equation in the form of a series in ϵ

$$r = S_0(\Phi) + \epsilon S_1(\Phi) + \dots \tag{13}$$

(after completing the calculations we should set $\epsilon = 1$). In our case

$$S_0(\Phi) = \kappa G^{-1}(\Phi - \theta), \tag{14}$$

$$S_1(\Phi) = -\frac{\kappa}{G'(G^{-1}(\Phi-\theta))} \arctan \frac{\kappa S_0(\gamma(\Phi))\sin\gamma(\Phi)}{E_{ex} + \kappa S_0(\gamma(\Phi))\cos\gamma(\Phi)}, \tag{15}$$

where $G^{-1}(.)$ is a function inverse to the function defined in (11); $\gamma(\Phi)$ is a multivalued function defined by the equation

$$\Phi = G(|E_{ex} + \kappa G^{-1}(\gamma-\theta)e^{i\gamma}|) + \theta. \tag{16}$$

Retaining only S_0 in Eq. (13) which corresponds to replacement of Φ^I_N in Eq. (10) by zero, we rewrite Eq. (13) in the form of a parametric equation of the curve of least detailed representation of SA, neglecting fine structure of any order

$$E = E_{ex} + \kappa\sqrt{v}\exp(iG(\sqrt{v}) + i\theta). \tag{17}$$

The NRR dynamics in such an approximation is determined by a 1-D mapping

$$v_{N+1} = E^2_{ex} + 2\kappa E_{ex}\sqrt{v_N}\cos(G(\sqrt{v_N}) + \theta) + \kappa^2 v_N \tag{18}$$

of curve (17) onto itself; here $v_N = r^2_N/\kappa^2$ (the zeroth approximation for mapping (9) was considered in Ref. [9]).

Retaining the terms S_0 and S_1 in Eq. (13) (linearization in Φ^I_N) we describe first-order fine structure. An enlarged segment of SA of mapping (9) for $E_{ex} = 6.73, \kappa = 0.15, R = \theta = -1$

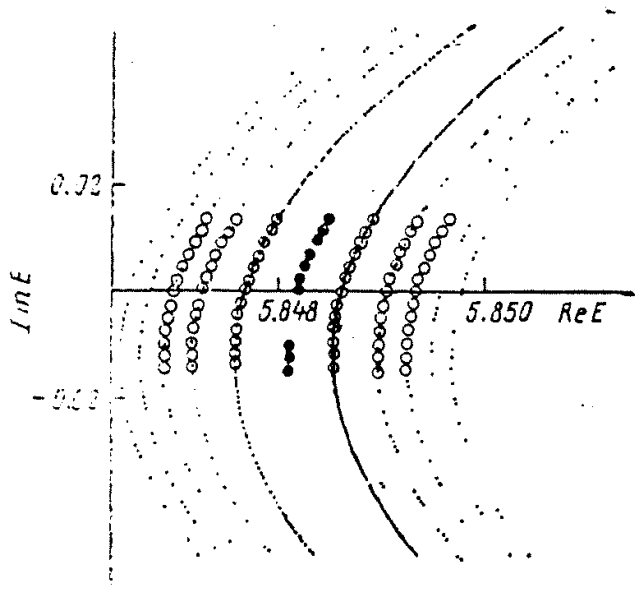

Figure 1: Fine structure of random attractor.

($|\Phi_N^I/\Phi_N^{II}| \sim 10^{-2}$ for these data) is shown in Fig. 1. The points correspond to results of numerical iterations; the initial point was chosen in curve (17) for $v = 11\pi$ [in the case of mapping (9), we should use $G(w) = R(1-w^2)$ in (17)]. The theoretical graph of SA in the zeroth (first) approximation is shown by solid (light) circles and agrees well with numerical results. We note that calculation is required of all orders in expansion (13) for exhaustive analytical description of the Cantor structure of SA; the resulting function is infinite-valued. Rearrangements of the attractors and corresponding threshold phenomena discussed in this paper are due to the existence of multicomponent attractors; each of components of such attractor has its own basin of attraction. We can observe in the numerical experiments both merging of the individual components taking place with variation of the controlling parameter and jumping of the phase trajectory from one component to the other, caused by impulse perturbations of the exciting wave. Using the approximate mapping (18) we illustrate how multicomponent attractor can emerge. A graph of the function (18) for $\nu = 2, E_{ex} = 1.05, \kappa = 0.33, R = 40$ and $\theta = 2.5$ is shown in Fig. 2. We can reproduce the iteration process graphically by drawing from any point of the curve horizontally to the intersection with the bisector of the angle between the axes, and from the intersection point found, vertically to the intersection with the mapping graph. We can see that the selection of the initial point in regions I, II or III leads to locking of the trajectory in the corresponding region; the trajectory never leaves this region (within the region, motion can be both regular and random). With arbitrary initial point, the trajectory is sooner or later will be trapped in one of these regions. Thus, in this case the attractor has three components. The condition of trapping can be violated by varying any of the parameters determining the shape of the curve (18) (fragments of the mapping graph are shown in the inlay of Fig. 2 for two situations: A–no trapping, B–trapping takes place). Changing the control parameter to lift the trapping condition, and then returning to the initial value, we can cause transition to another component. For $|\Phi_N^I/\Phi_N^{II}| \ll 1$, mappings (8) (exact 2-D) and (18) (approximate 1-D) have multicomponent attractors for close values of the parameters. Hence, it is convenient in the search of such attractors to begin study of the 1-D mapping that shows the appropriate combinations of parameters, and only after this, proceed to the numerical iteration

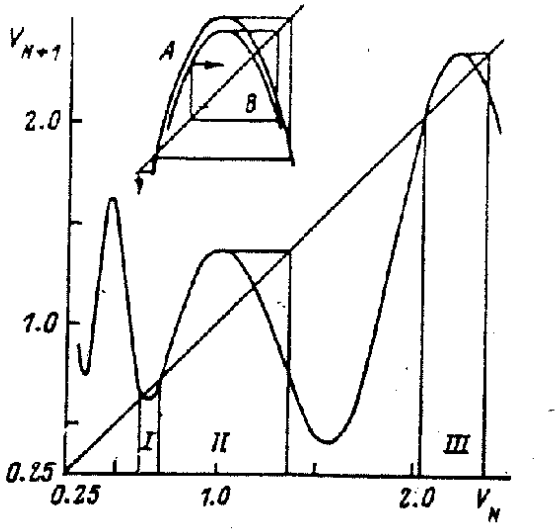

Figure 2: Approximate 1-D mapping (18) in the case of two-photon transitions.

of mapping (8). Same results obtained this way are tabulated. Mapping (8) was iterated for $\nu = 2, E_{ex} = 1, R = 18$, and different κ and θ). Each group of three symbols, containing (not containing) the point, characterizes a two-component (three-component) attractor; the point replaced the symbol of the component, for which the locking condition ceases to be satisfied (phase trajectory is locked by the adjacent component). In order to characterize the dynamics within one component, we use the notation: S means stationary point; 2, 4, 8 stand for cycles of corresponding multiplicity; X – randomness; $\underline{X}$ – randomness with a double-cycle structure (the latter means that the group of points with even and odd numbers have close and distant regions of localization from one another, but, on the whole, the motion is random).

θ												
	X$\underline{X}$S	X$\underline{X}$S	.$\underline{X}$S	.$\underline{X}$S	.$\underline{X}$S	.$\underline{X}$S	.$\underline{X}$S	.$\underline{X}$S	.$\underline{X}$S	.$\underline{X}$S	.$\underline{X}$S	.$\underline{X}$S
3.375	$\underline{X}\underline{X}$.	X$\underline{X}$S	X$\underline{X}$S	X$\underline{X}$S	.$\underline{X}$S	.$\underline{X}$S	.$\underline{X}$S	.$\underline{X}$S	.$\underline{X}$S	.$\underline{X}$S	.$\underline{X}$S	.$\underline{X}$S
	$\underline{X}\underline{X}$.	$\underline{X}\underline{X}$.	$\underline{X}\underline{X}$S	X$\underline{X}$S	X$\underline{X}$S	.$\underline{X}$S	.$\underline{X}$S	.$\underline{X}$S	.$\underline{X}$S	.XS	.XS	.XS
3.350	4$\underline{X}$.	4$\underline{X}$.	8XS	$\underline{X}\underline{X}$S	XXS	XXS	XXS	.XS	.XS	.XS	.XS	.XS
	4X.	4X.	4X.	4XS	$\underline{X}$XS	XXS	XXS	XXS	.XS	.XS	.XS	.XS
3.325	2X.	2X.	2X.	4X.	4XS	8XS	$\underline{X}$XS	XXS	XXS	XXS	.XS	.XS
	2X.	2X.	2X.	4X.	4X.	8XS	4$\underline{X}$S	$\underline{X}$XS	XXS	X.S	X.S	.XS
				0.56				0.565				κ

Numerical modeling of the dynamics of mapping often leads to results hardly amenable to interpretation. It is difficult to distinguish the complex periodic motion from the random or one type of randomness to another. In this situation, it is convenient to use additional information, including dependence of the maximum Lyapunov index (MLI) [10] on some system parameter. The MLI characterizes the rate of divergence (convergence) of close phase trajectories, averaged along a certain trajectory, and can be found numerically; the MLI is positive for random

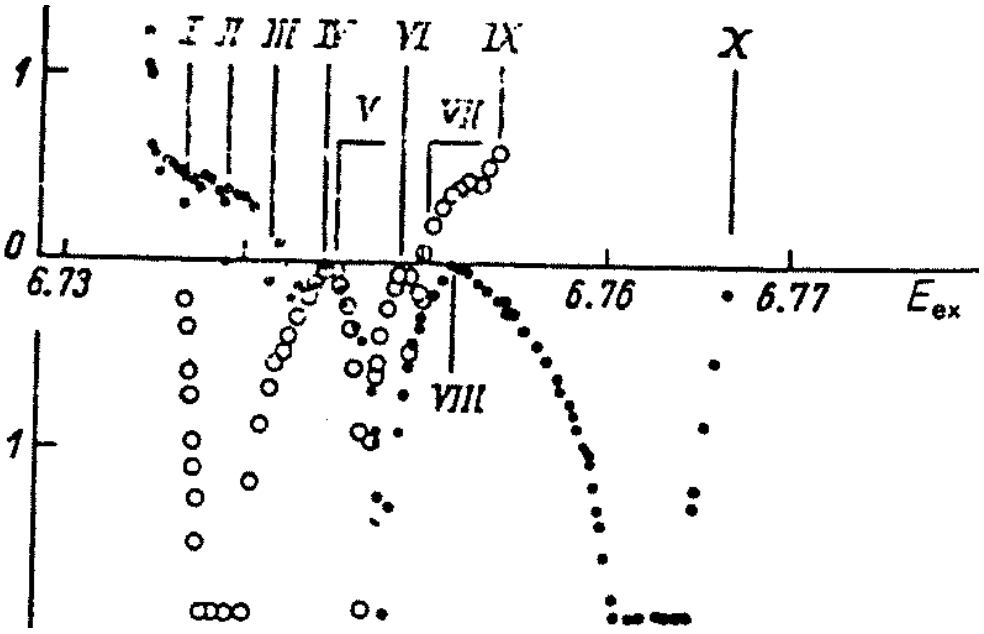

Figure 3: Dependence of maximum Lyapunov index on exciting field amplitude.

motion, and negative for stationary point or limiting cycle. In our case, calculation of the MLI allows us to obtain detailed information on variation of the structure of the attractor in the rearrangement region. Dependence of the MLI L on E_{ex}, for mapping (9) ($R = \theta = -1, \kappa = 0.15$) is shown in Fig. 3. A two-component attractor exists in the regions I-IX; variations corresponding to the various components are shown by points and circles. We observe for each of them transition of randomness according to the Feigenbaum scenario [11] the E_{ex} values for which cycles of multiplicities 2 and 4 and randomness arise are denoted by numerals V, VI, VII (circles) and VIII, IV, III (points). The dependence of MLI for a one-component attractor is shown by points to the left of I and right of IX, The transition between stationary point and randomness is denoted by the numeral X, while the window of stability in the random zone by numeral II. We can assume that threshold phenomena and multistability are due to rearrangement of attractors, and this is one of the typical scenarios of behavior of a nonlinear system with delay (elementary scenarios of onset of randomness are given in Ref. [12]). A crisis randomness described in Ref. [13] is associated with this scenario. Study of the means of altering SA and search for scenarios is of definite interest in connection with prospects of the design of optical logic devices and computer memory cells. We note that rearrangements of attractors in systems with continuous time and in the distributed systems were discussed in Ref. [14]. Some other threshold effects in systems with SA leading to typical dependence of MLI on the parameter are considered in Ref. [15].

References

[1] K. Ikeda, H. Daido, and O. Akimoto, Phys.Rev.Lett. **45**, 709 (1980).

[2] R. R. Snapp, H. J. Carmichael, and W. C. Schieve, Opt.Commun. **40**, 68 (1981).

[3] Singh Surendra and G. S. Agarwal, Opt.Commun. **47**, 73 (1983).

[4] R. G. Harrison, W. J. Firth, C. A. Emsbary, and I. A. Al-Saidi, Phys.Rev.Lett. **51**, 562 (1983).

[5] H. Nakatsuka, S. Asaka, H. Itoh, K. Ikeda, and M. Matsuoka, Phys.Rev.Lett. **50**, 109 (1983).

[6] R. Bridges and G. Rowlands, Phys.Lett. **A63**, 189 (1977);
Y. Yamaguchi and N. Mishima, Phys.Lett. **A104**, 179 (1984).

[7] *Strange Attractors*, Mir Publishers, Moscow (1981).

[8] V. V. Zverev, and B. Y. Rubinshtein, in *Proceedings of 3rd Symposium on Light Echo and Coherent Spectroscopy: Abstracts of Reports* (Kharkov, 1985), p. 85.

[9] J. Carr and J. C. Eilbeck, Phys.Lett. **104A**, 59 (1984).

[10] A. Lichtenberg and M. Liberman, *Regular and Stochastic Dynamics* (Moscow, 1984).

[11] M. J. Feigenbaum, J.Stat.Phys. **19**, 25 (1978).

[12] J. P. Ekman in *Synergetics* (Moscow, 1984), p. 190.

[13] C. Grebogi, and J. A. Jorke, Phys.Rev.Lett. **48**, 1507 (1982); M. Kitano, T. Yabuzaki, and T. Ogawa, Phys.Rev. **A29**, 1288 (1984).

[14] I. S. Aranson, M. I. Rabinovich, and M. Starobinets in *Problems of Nonlinear and Turbulent Processes in Physics, Proceedings of 2nd International Working Group, Part 2* (Kiev, 1985), p. 3.

[15] H. Daido, Phys.Lett. **108A**, 233 (1985);
H. Daido, and H. Haken, Phys.Lett. **111**, 211 (1985).